Heat and Technology
Vol. 32, n. 1-2, 2014

THREE-DIMENSIONAL SIMULATION OF THE THERMAL PERFORMANCE OF POROUS BUILDING BRICK IMPREGNATED WITH PHASE CHANGE MATERIAL

Nidhal Ben Khedher *, Sassi Ben Nasrallah

Email: nidhal.ben.khedher@gmail.com

*Université de Monastir, École Nationale d'Ingénieurs de Monastir, Laboratoire d'Études des Systèmes Thermiques et Énergétiques LESTE, Avenue Ibn El Jazzar 5019, Monastir, TUNISIE

ABSTRACT

Integration of phase change materials (PCMs) into building fabrics is considered to be one of the potential and effective ways of minimizing energy consumption and CO2 emissions in the building sector. The application of such materials for building construction makes it possible to improve thermal comfort in summer and reduce heating energy consumption in winter. The choice of a PCM depends deeply on the building structure, on the weather and on building use: numerical modelling is indispensable. The thermal performances of a brick impregnated with PCM (PCM-brick) have been numerically investigated in a full scale test room. The PCM-brick is assumed to be a porous medium saturated with PCM. Three-dimensional model is developed to asses the thermal behaviour of this porous medium (PCM-brick). The volume averaged energy equation with phase change in the porous medium is discretized by the control volume finite element method (CVFEM). The resulted algebraic equation was solved by the Bi-Conjugate Gradient Stabilized iterative solver. A series of numerical tests are then undertaken to assess the effects of PCM type, matrix porosity and brick thickness on the indoor air temperature for three summer days.

INTRODUCTION

Integrating phase change materials (PCM) into building walls is a potential method for reducing energy consumption in passively designed buildings. An interesting feature is that they can store latent heat energy, as well as sensible energy. As the temperature increases, the material changes phase from a solid to a liquid. As this physical reaction is endothermic, the PCM absorbs heat. Similarly, when the temperature decreases, the material changes phase from a liquid to a solid. As this reaction is exothermic, the PCM releases heat.

Over the past decade, the integration of phase change materials (PCMs) into building elements such as walls, ceilings and floors has been investigated as a potential technology for passive solar thermal storage. This technique has the following advantages: the PCM composites can offer high thermal storage capacity over a narrow temperature range; the PCM building elements provide large heat transfer area and they can be easily produced and installed with existing facilities. Many of these PCM composites (such as PCM-gypsum board[1], PCM-concrete board, etc...) are prepared by immersing wallboard into PCM or by direct incorporation at the mixing stage of wallboard production.

Reviews of principles, of available PCMs and expected applications were made by a significant number of authors and we can cite the publications of Hasnain [2] and Zalba et al. [3]. Concerning the use of PCM in building materials, a methodology for choosing a PCM has been developed by Peippo et al. [4] for passive solar heating and criteria of choice were given by Gu et al. [5] for thermal energy recovery with air-conditioning systems. The use of PCM materials for construction has been a subject of considerable interest in the last decade.

The simplest way of incorporating phase change substances into building materials is by immersion. The porous building material is dipped into the hot melted PCM, which is absorbed into the pores by capillary suction. Then material is removed from the liquid PCM and allowed to cool and the PCM remains in the pores of the building material. H. Kaasinen [6] has looked at the absorption of certain organic PCMs into a wide range of building materials including wallboards, timber and brick.

Athienitis et al. [7] performed an experimental investigation of gypsum board impregnated with a phase change material in a direct-gain outdoor test-room. The results showed that the use of PCM-gypsum board in a passive solar building may reduce the maximum room temperature by about 4 °C during the daytime and can reduce the heating load at night. Stovall and Tomlinson [8] analyzed the PCM wallboard for load management and to enhance comfort. Their results showed that the wallboard was ineffective in modifying the comfort level but did provide significant load management relief. Ahmad et al. [9]'s study also showed that the impact of PCM was remarkable with a reduction of the indoor air temperature amplitude in the light-weight test-cell.

Recently, Takahiro Nomura et al. [10] studied the impregnation of a porous material with a phase change material; erythritol was selected as the PCM and expanded perlite, diatom earth (DE), and gamma-alumina (GA) were selected as porous materials. Effects of vacuum in impregnation, pore size of porous materials, holding time and

cyclic test on thermal properties of composites; latent heat, melting temperature, were mainly examined by using DSC.

In this study, thermal analyses of a three-dimensional model for a porous building brick containing phase change material are presented. A serial of numerical calculations have been performed in order to analyze the potential of the PCM-brick. When selecting a PCM, the average room temperature should be close to the melting/freezing temperature range of the material. Moreover, the day fluctuations should allow the material phase change. Then many factors influence the choice of the PCM: weather, building structure and thermophysical properties Numerical simulation must then be used to achieve the practical application of this technology. So the influences of the PCM type and PCM-brick porosity have been studied.

2. MODELLING

2.1 Mathematical model

The system considered in this work is a brick assumed to be a porous medium composed of an inert and rigid solid phase (brick matrix), initially saturated with a phase change material.

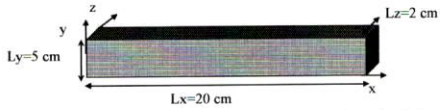

Fig.1 Representation of the PCM brick

Governing equations

In this work we focus on the heat exchange between the porous PCM brick and the surrounding environment.

The porous medium is a brick matrix filled with the phase change material (PCM). The considered porous medium is undergoing phase-change. The following simplifying assumptions are made in the analysis:

- The porous layer is homogenous and isotropic.
- The porous matrix and the phase change material are in local thermal equilibrium
- The volume change caused by freezing is negligible.
- All thermophysical properties of all phases are independent of temperature but they differ from phase to another.
- Conduction is the driven heat transfer mechanism for the latent thermal energy storage systems (V.Alexiades et al. [11], J.P. Trelles et al. [12]).

The governing partial differential equations describing the phase change of the porous medium are obtained from the volume averaging of the main conservation equations energy.

✓ Energy conservation equation

$$\frac{\partial}{\partial t}\left(\rho C_p T\right) = \nabla\left(\lambda_{eff}.\nabla T\right) - \rho_l L_H \varepsilon \frac{\partial f}{\partial t} \qquad (1)$$

Considering the isothermal phase change, the liquid fraction is updated iteratively at each control volume P using this formula (Voller [13])

$$f^{k+1} = f^k + \frac{A_p\left(T_p - T_m\right)}{\rho_l L_H \varepsilon}, \quad \text{with the restriction}$$

$$f^{k+1} = \begin{cases} 1 & \text{if } f^{k+1} > 1 \\ 0 & \text{if } f^{k+1} < 0 \end{cases} \qquad (2)$$

using this formula : where is the coefficient that appears in the discretized energy equation and is the melting temperature.

✓ Thermodynamic relations

The average density and specific heat are defined as :

$$\rho = \sum_k \varepsilon_k \rho_k \quad C_p = \frac{1}{\rho}\sum_k \varepsilon_k \rho_k C_k \qquad (3)$$

Also, L_H is the latent heat of melting of the PCM.

For the effective thermal conductivity λ_{eff} the weighted conductivity model (or parallel resistance model) defined below is employed.

$$\lambda_{eff} = \sum_k \varepsilon_k \lambda_k \qquad (4)$$

External conditions

The outdoor side of the wall is subjected to a time dependent radiation and forced convection boundary conditions, with h_o=20 W/m °C. At the indoor surface, a free convection boundary condition, with hi=10 W/m °C. The heat flow into the outdoor wall can be expressed as:

$$Q_{os} = Q_{conv} + Q_s - Q_{Correc} \qquad (5)$$

Or

$$Q_{os} = h_o A\left(T_o - T_{os}\right) + \alpha A q_s - \varepsilon A\sigma\left(T_o^4 - T_{surr}^4\right) \qquad (6)$$

where To is the outdoor air temperature, Tos the outdoor surface temperature, α the solar absorptivity of the wall surface, and qs is the solar flux radiation. The last term in Eq. (6) represents the correction for the radiation heat transfer when the surrounding and the ambient temperatures are not equal. It is assumed that these two temperatures are equal in this study. The heat flow into the outdoor surface can be expressed as:

$$Q_{os} = h_o A\left(T_s - T_{os}\right) \qquad (7)$$

where Ts is the solar-air temperature, which is defined as:

$$T_s = T_o + \alpha \frac{q_s}{h_o} \qquad (8)$$

Boundary and initial conditions

Initially, the temperature and liquid fraction are uniform in the porous medium.

$$\overline{T}\left(x, y, z, t = 0\right) = T_0 \,, f\left(x, y, z, t = 0\right) = f_0 \qquad (9)$$

The boundary condition a the indoor surface (y=0)

$$-\lambda \frac{\partial \overline{T}}{\partial y} = h_i\left(T_i - T_{is}\right) \qquad (10)$$

where Tis is the indoor surface temperature.

The boundary condition a the outdoor surface (y=L)

$$-\lambda \frac{\partial \overline{T}}{\partial y} = h_o\left(T_s - T_{os}\right) \qquad (11)$$

On the adiabatic and impervious sides, the heat fluxes are equal to zero.

At z=0 and z=Lz :

$$\frac{\partial \bar{T}}{\partial z} = 0 ,$$

At x=0 and x=Lx :

$$\frac{\partial \bar{T}}{\partial x} = 0 ,$$

Model of the indoor air:

The energy conservation equation for the indoor air is:

$$\rho_a C_p V_R \frac{dT}{dt} = \sum_{i=1}^{N} Q_{w,\text{in}} + Q_{s,in} + Q_{Leakage} + Q_{win} \quad (12)$$

where V_R represents cubage of the room, Qw,in the convection heat transfer rate between air and inner surfaces of the room, $Q_{s,c}$ the convection heat transfer rate from the indoor heat source, QL the heat transfer rate by air leakage, and Q_{win} the heat transfer rate through the window. $Q_{w,i}$, Q_L and Q_{win} are calculated by the following equations:

$$Q_{w,\text{in}} = h_i \times (T_{w,i} - T_i) \times A_{w,i} \quad (13)$$

$$Q_{win} = A_{win} \times (T_o - T_i) \times U_{win} \quad (14)$$

$$Q_{Leakage} = \rho_a C_p V_R \times ACH \times (T_o - T_i) \quad (15)$$

$$Q_{s,in} = \sum_{i=1,nbt} P_i \quad (16)$$

where Tw,i is the inner surface temperature of a wall, ceiling and floor while Aw,i is its area. Uwin and Awin are overall heat transfer coefficient and the area of the window respectively. Pi is the heat generation rate by the equipment.

3. NUMERICAL TREATMENT

The equations set, with initial and boundary conditions have been solved numerically using the control volume finite element method (CVFEM) (Saobas [14], Ben Khedher [15] Grissa [16]). The advantages of this method are (i) It ensures the flux conservation (ii) the used control volumes present more faces, that makes it possible to avoid the numerical diffusion. (iii) The control volume is composed of triangular elements which improve the grid flexibility

The 3D discretization of the physical domain consists in dividing the plane (x,y) into three-node triangular elements. Then the centroids of these elements are joined to the midpoints of the corresponding sides. This creates the polygonal control volumes around each node in the finite element grid. At this level the 3D discretization is similar to 2D one. But for the 3D discretization we complete the construction of the control volume by employing the finite-volume method along the third direction (z).

The governing equations cited before could be written in the following form:

$$\frac{\partial (f_1 \Phi)}{\partial t} + \text{div}(\vec{J}_\Phi) = S_\Phi \quad (17)$$

With the vector $\vec{J}_\Phi$, representing combined convection and diffusion flux of the dependent variable Φ $(\bar{T}, T_f)$ given by

$$\vec{J}_\Phi = f_2 \vec{U} \Phi - \Gamma_\Phi \overrightarrow{\text{grad}}\, \Phi \quad (18)$$

Γ_Φ, $\vec{U}$ and S_Φ are respectively diffusion coefficient, the velocity vector and the source term.

The control volume is composed of six sub-volumes Ω_b (Fig.3) with equal sizes.

$$\int_t^{t+\Delta t} \int_{V_c} \left(\frac{\partial (f_1 \Phi)}{\partial t} + \text{div}\vec{J}_\Phi - S_\Phi \right) dV_c\, dt = \int_t^{t+\Delta t} \sum_{\Omega_b} \int_{\Omega_b} \left(\frac{\partial (f_1 \Phi)}{\partial t} + \text{div}\vec{J}_\Phi - S_\Phi \right) d\Omega_b\, dt = 0 \quad (19)$$

Instead of integrate over all sub-volumes; we work simply on one sub-volume Ω_b.

The integration of Eq. (13) over the sub-volume (Ω_b), using the divergence theorem and the implicit procedure, leads to:

$$\int_{\Omega_b} \frac{(f_1 \Phi)^{n+1} - (f_1 \Phi)^n}{\Delta t} d\Omega_b + \int_\Gamma \vec{J}_\Phi^{\,n+1} . \vec{n}\, d\Gamma = \int_{\Omega_b} S_\Phi^{n+1} d\Omega_b \quad (20)$$

where Δt is the time step, the subscripts n and n+1 refer to a previous instant t and the latest instant t+Δt, and $\vec{n}$ denotes the outward pointing normal vector on the control volume surface Γ.

For the reason of simplification the control volume surface can be divided into simple surfaces with easily determined normal vectors.

So the integration of the vector of flux over the control volume surface Γ (Fig. 2) can be written in this way:

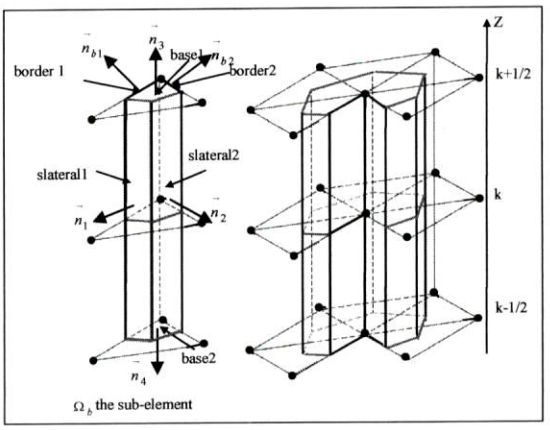

Fig. 2 Control volume and sub-volume

$$\int_\Gamma \vec{J}_\Phi^{\,n+1} . \vec{n}\, d\Gamma = \iint_{slateral1} \vec{J}_\Phi^{\,n+1} . \vec{n}_1\, dS + \iint_{slateral2} \vec{J}_\Phi^{\,n+1} . \vec{n}_2\, dS + \iint_{base1} \vec{J}_\Phi^{\,n+1} . \vec{n}_3\, dS + \iint_{base2} \vec{J}_\Phi^{\,n+1} . \vec{n}_4\, dS + [\text{limit}] \quad (21)$$

with $[\text{limit}] = \iint_{border1} \vec{J}_\Phi^{\,n+1} . \vec{n}_{b1}\, dS + \iint_{border2} \vec{J}_\Phi^{\,n+1} . \vec{n}_{b2}\, dS$

For an interior node the term $[\text{limit}]$ of all sub-volumes is equal to zero. Otherwise, we should take boundary conditions into account in order to calculate this term.

We have chosen a linear interpolation of Φ in order to calculate the flux term across the control volume faces. The resulting algebraic system from assembling the contributions of all sub-volumes has the following general form:

$$A_P \Phi_P^{n+1} = \sum_{nb} A_{nb} \Phi_{nb}^{n+1} + B^{\Phi} \quad (22)$$

The subscripts P and nb denote respectively the principal node and the neighbouring nodes. The resulting algebraic system has been solved iteratively by SSOR-preconditioned BICGSTAB (Bi-Conjugate Gradient Stabilized) (Y. Saad [17]) algorithm which has been implemented in FORTRAN computer code.
each page.

4. RESULTS AND DISCUSSIONS

The effectiveness of the PCM_brick is evaluated by representing the indoor temperature evolution during three days of summer (July 2013) of a typical room which lies in Tunisian southern city (Gafsa). The dimension of the room is taken as 5.0m (length)×3.0m (width)×3.0m (height). The room walls are built from PCM brick (brick impregnated with PCM). The dimensions of this porous brick are represented in Fig.1. The total indoor heat generation rate by the equipment, light and occupants etc. is assumed to be 100W.
The typical day weather of July in the Tunisian southern city of Gafsa, is chosen as the outdoor climate data. The hourly variation of outdoor air temperature and solar radiation is shown in Fig.3. Table 1 lists the main parameters of the room studied.

Table1: Main parameters of the room.

ACH h^{-1}	A_{win} m^2	U_{win} $(W/m^{2o}C)$	$Q_{s,in}$ W
1	2.25	2.68	100

4.1 Effect of PCM type

Fig. 4 shows the room air temperature profile for three PCM types. The melting temperature of these three PCM is within the operating temperature of the system. Calcium chloride hexahydrate (CaCl26H2O), n-Eicosane, n-Octadecane are investigated as potential PCMs. The thermal properties of these PCMs are depicted in table 2. The outdoor temperature of the typical summer day swings between 23°C and 50°C. The indoor air temperature for ordinary brick without PCM is close to the exterior temperature with a little time lag due to the low thermal inertia of the room. It is clearly noticed that the PCM included in the bricks reduces the temperature fluctuations in the room. The melting temperatures of n-Octadecane and Calcium chloride hexahydrate (CaCl26H2O) are close to the lower limit of the operating temperature, while the melting temperature of n-Eicosane is almost at the middle of

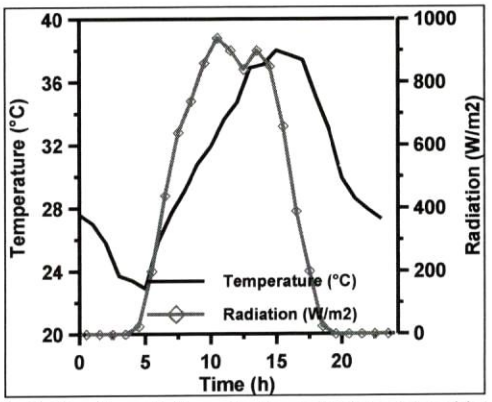

Fig. 3 Hourly variation of solar radiation and ambient temperature for a typical day of the month of July 2009 for Tunisian southern city (Gafsa)

temperature limits. It is shown that n-Eicosane brick performs thermally better than the other two types of the PCM-bricks. The indoor temperatures of CaCl26H2O and n-Octadecane PCM-bricks are very close to the case of ordinary brick (without PCM). Their low melting temperature made them in liquid phase all the time. They absorb the heat and melt during the first sunny period and they stay at this liquid state. The Eicosane is the proper PCM type was obtained by choosing the narrowest swing of the indoor air temperature among the cases with the different PCM types. The use of Eicosane-brick engenders the decreasing of the maximum air temperature value of about 3 °C and the decreasing of the minimum air temperature of about 1°C.

Table 2: Thermal properties of brick and PCMs

Material	T_m (°C)	λ (W/m°C)	C_P (kJ/kg°C)	ρ (kg/m3)	$L_{H\,MCP}$ (kJ/°c)
Porous brick	_	0.7	0.84	1600	-
n- Octadecane	27	0.385(solid), 0.148(liquid)	1.934(solid), 2.196(liquid)	865 solid 780 liquid	243.5
n-Eicosane	37	0.15 (solid), 0.15 (liquid)	2.01 (solid), 2.04 (liquid)	778 solid 856 liquid	241
$Cacl_2$6H2O	29	1.09 (solid), 0.54 (liquid)	2.4 (solid), 2.04 (liquid)	1710 solid 1500 iquid	164

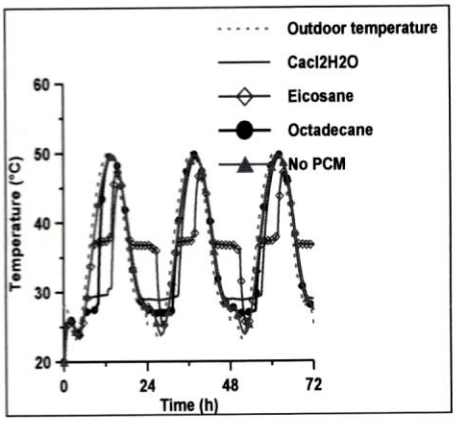

Fig.4 Simulated hourly indoor air temperature for various types of PCM

To further understand the behaviour of the Eicosane brick, we presented the temperature and the saturation distributions for the porous Eicosane-brick at different instants of the first day (Fig. 5, Fig. 6). It can be seen that the porous medium (brick) melts and absorbs heat coming from outdoor during the daytime. Then during the night period the porous medium releases the previously stored heat and solidifies. Here we can distinguish two periods storage period (melting) (Fig.5) and discharging one (solidification) (Fig.6).

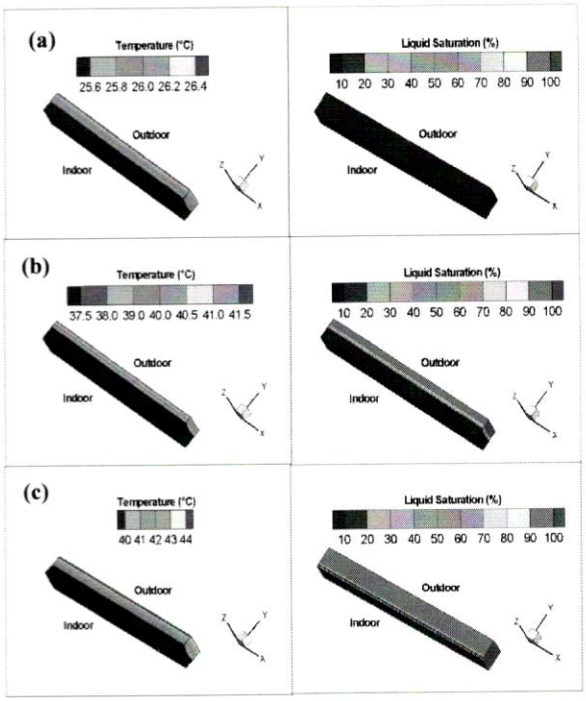

Fig. 5. Temperature and saturation fields (PCM melting), (a) 6h, (b) 10h, (c) 13h

These two periods are obviously indicated in Fig.7 where we depicted the history of latent heat, sensible heat and total heat stored in the PCM-brick. Over a day the solar energy is stored in the material (melting process).The heat is released during the night when the zone's resultant temperature drops below the solidification temperature (solidification process). Fig.7 shows also that the larger amount of stored heat by the PCM-brick is a latent heat, which proves the quality of the phase change materials.

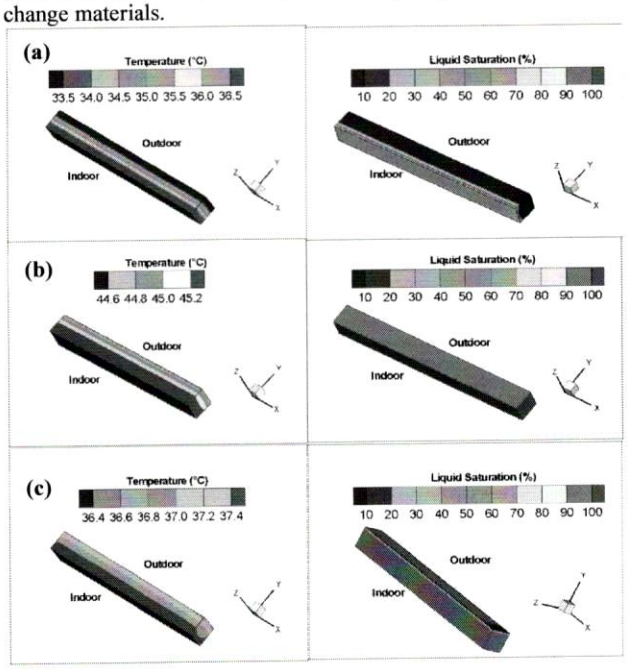

Fig.6 Temperature and saturation fields after (solidification),(a)16h, (b) 20h, (c) 24h

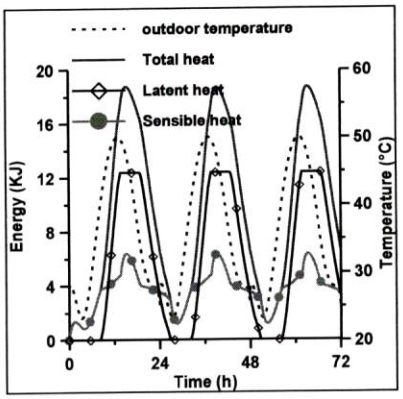

Fig. 7. Stored energy in the PCM brick (PO=0.5, Ly=2cm)

4.2 Effect of brick matrix porosity

The PCM-brick is obtained by impregnating porous brick with PCM. So the PCM quantity is tightly linked to the porosity of the brick. Then increasing porosity means raising PCM quantity. It is noticed from Fig. 8 that increasing porosity reduces the swing of the indoor temperature. For ε=0.2 the indoor temperature swing is quite high and it approaches the case of ordinary brick (No PCM). This behaviour is justified by the fact that for small porosities there is not enough PCM to store heat. However, for ε=0.8 the lowest limit of the indoor temperature is equal to the melting temperature of the PCM. So the melted PCM quantity during the storage period does not entirely solidify and there is PCM which remains in the liquid phase. The porosity is an important parameter that must be

optimized to guarantee that the whole PCM's latent heat is used and the cost of the PCM-brick is reduced.

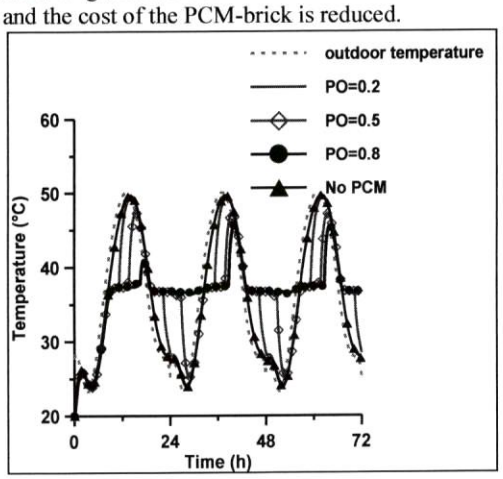

Fig. 8. Simulated hourly indoor air temperature for various brick porosities for Eicosane PCM-brick

4.3 Effect of PCM-brick thickness

Thickness of PCM-brick is also an important parameter of influencing its thermal performance. Fig. 9 shows that for L=1cm the indoor air temperature almost equal to the outlet temperature. That is due to the poor inertia of the building; the weak thermal capacitance of the PCM-brick; and to the too small PCM quantity. By increasing the PCM-brick thickness the thermal performance is improved, because the PCM quantity and the building inertia are raised. For L=5cm the indoor temperature is maintained almost equal to the melting temperature. This result is fascinating because for an outdoor temperature equal to 50°C we have an indoor temperature of 37°C. But we have to guarantee the melting and the solidification of the whole PCM. Otherwise we are spending money for extra PCM quantity to ensure the thermal isolation of the room without taking advantage of its latent heat of fusion. Moreover for high PCM-brick thickness and for high amount of indoor generated heat, this heat could not be easily evacuated outside. So the heat will be stored in the PCM-brick to be released during the night period.

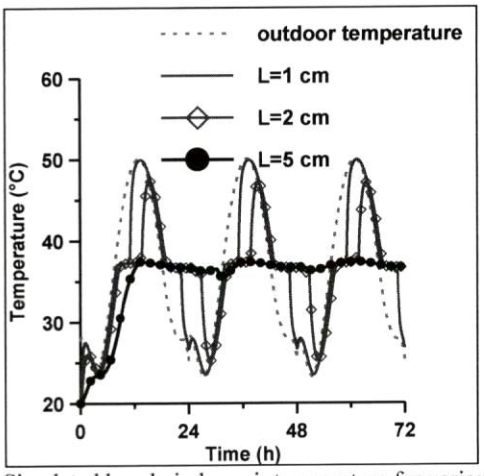

Fig. 9. Simulated hourly indoor air temperature for various PCM/brick thickness

5. CONCLUSION

In this paper a three-dimensional simulation is put forward to evaluate the thermal performance of brick impregnated with PCM in a passive building in Tunisian southern region. The following conclusions can be made from this numerical study:
1- The use of phase change material in bricks allows the enhancement of the thermal performance of buildings. Since including the PCM wallboard reduces the indoor air temperature fluctuations by absorbing the outdoor heat during the sunny period and releasing it at night.
2- In order for its use with an optimal storage effect during a complete day, the PCM type (melting temperature, latent fusion heat,…), the PCM-brick porosity and thickness must be optimized.
3- For the purpose of narrowing indoor air temperature swing, the suitable melting temperature of PCM is roughly equal to the average indoor air temperature of summer days.
4- The porosity is an important parameter must be optimized to guarantee that the whole PCM's latent heat is used and hence the cost of the PCM-brick is reduced.6.

6. NOMENCLATURE

ACH	air change per hour [h-1]
Cp	constant specific heat [J/(Kg.K)]
f	Liquid fraction
g	gravitational constant [m/s2]
h_{in}	indoor heat transfer coefficient [W/(m².K)]
h_o	outdoor heat transfer coefficient [W/(m².K)]
L_H	fusion latent heat [J / Kg]
Lx	porous PCM brick length
Ly	porous PCM brick width
Lz	porous PCM brick thickness
$\overline{T}$	Average temperature [K]
T_0	initial temperature [K]
t	time [s]
U	overall heat transfer coefficient [W/m2°C]
Δt	time step

Greek symbols

ε	Porosity
λ	Thermal conductivity [W/(m.K)]
ρ	Density [Kg/m3]

Subscripts

eff	effective
in	indoor
l	liquid
o	outdoor
win	window
s	solid
x,y,z	Cartesian coordinates
0	initial

7. REFERENCES

1. D. Feldman, D. Banu, DW. Hawes, Development and application of organic phase change mixtures in thermal storage gypsum wallboard. Solar Energy Mater Solar Cells, vol 36, 147–57,1995.

2 S.M. Hasnain, Review on sustainable thermal energy storage technologies, Part I: heat storage materials and techniques, Energy Research, vol 39, 1127–1138,.1997.

3 B. Zalba, J.M.Marin, L.F. Cabeza, H.Melhing, Review on thermal energy storage with phase change materials, heat transfer analysis and applications, Applied Thermal Engineering, vol. 23, 251–283, 2003.

4 K. Peippo, P. Kauranen, P.D. Lund, A multicomponent PCM wall optimized for solar heating, Energy and Buildings, vol. 17, 259–270, 1991.

5 Z. Gu, H. Liu, Y. Li, Thermal energy recovery of air conditioning system—heat recovery system calculation and phase change materials development, Applied Thermal Engineering, vol. 24,pp 2511–2526, 2004.

6 Kaasinen H., The absorption of phase change substances into commonly used building materials, Solar Energy Materials and Solar Cells, vol 27,pp 173-179, 1992.

7 Athienitis AK, Liu C, Hawes D, Banu D, Feldman D. Investigation of the thermal performance of a passive solar test-room with wall latent heat storage. Building Environment, vol 32, pp 405–10, 1997.

8 Stovall TK, Tomlinson JJ. What are the potential benefits of including latent storage in common wallboard? J Solar Energy Eng Trans ASME, 117(4), pp 318–25, 1995.

9 Ahmad M, Bontemps A, Sall H, Quenard D. Thermal testing and numerical investigation of a prototype cell using light wallboard coupling vacuum isolation panels and phase change material. Energy Build;38:673–81, 2006.

10 Takahiro Nomura, Noriyuki Okinaka, Tomohiro Akiyama, Impregnation of porous material with phase change material for thermal energy storage, Materials Chemistry and Physics 115, pp.846–850, 2009.

11 V.Alexiades, A.D. Solomon, Mathematical Modeling of Melting and Freezing Processes, Hemisphere Publishing Corporation, 1993

12 P. Jyan Trelles, John J. Dufly, "Numerical simulation of porous latent heat thermal energy storage for thermoelectric cooling", Applied Thermal Engineering , vol 23, pp.1647-1664, 2003.

13 V. R. Voller, Fast implicit finite-difference method for the analysis of phase change problems, Numerical Heat Transfer, Part B,vol 17, pp.155-169, 1990.

14 Saobas HJ, Balliga BR, Collocated equal order control volume finite-element method for multidimensional, incompressible fluid flow, Part I: formulation. Numerical Heat Transfer B;vol. 26, pp 14-07, 1994.

15 N. Ben khedher, S. Ben Nasrallah. Unstructured control volume finite element method for coupled heat and mass transfer during the drying of porous medium having complex 2d-geometry, International Journal of Heat & Technology, vol. 28, n. 2,pp.79-88, 2010.

16 H. Grissa, F. Askri, M. Ben Salah, S. Ben Nasrallah, Coupled conduction-radiation heat transfer problem for three-dimensional complex geometry, International Journal of Heat & Technology, vol 29, No 2, 2011.

17 Y. saad (1996), iterative methods for sparse linear systems, PWS Publishing Company.